RSC Advances

PAPER

View Article Online
View Journal | View Issue

Cite this: *RSC Adv.*, 2022, **12**, 4595

Study of the preparation of Maifan stone and SRB immobilized particles and their effect on treatment of acid mine drainage

Xuying Guo, *[ab] Zhiyong Hu, [a] Yanrong Dong,[c] Saiou Fu[c] and Ying Li[d]

The problems of acid mine drainage (AMD) in coal mine acidic wastewaters arise from a range of sources, including severe pollution with heavy metals and SO_4^{2-} and difficulties during treatment. Based on the ability of Maifan stone to adsorb heavy metals and the dissimilatory reduction of SO_4^{2-} by sulfate-reducing bacteria (SRB), Maifan stone–sulfate-reducing bacterium-immobilized particles were prepared *via* immobilization techniques using Shandong Maifan stone as the experimental material. A single factor experiment was used to investigate the influences of the dosage of Maifan stone, the particle size of Maifan stone and the dosage of SRB on the pH improvement effect and the removal rates of SO_4^{2-}, Fe^{2+} and Mn^{2+}. The Box–Behnken response surface method was used to determine the optimal preparation conditions for the Maifan stone and SRB immobilized particles in accordance with the ion removal rate and pH improvement effect when dealing with AMD. The results show that: (1) the optimal preparation conditions for Maifan stone synergistic SRB immobilized particles are determined by single factor experiment: the dosage of Maifan stone is 5 g, the particle size of Maifan stone is 0.075–0.106 mm, and the dosage of SRB is 25 mL per 100 mL; the removal rates of SO_4^{2-}, Fe^{2+} and Mn^{2+} from AMD by the Maifan stone and SRB immobilized particles prepared under these conditions were 92.22%, 95.41% and 86.05%, and the pH was increased from 4.08 to 7.45. (2) From the variance analysis of the response surface model, it can be seen that the model effectively predicts the SO_4^{2-} removal rate, Fe^{2+} removal rate, Mn^{2+} removal rate and pH change. (3) After further optimization using the response surface method, the optimal preparation conditions of Maifan stone and SRB immobilized particles are determined as follows: Maifan stone dosage is 5 g, Maifan stone particle size is 0.075–0.106 mm, and SRB dosage is 25 mL per 100 mL. Through experiments, the removal rates of SO_4^{2-}, Fe^{2+} and Mn^{2+} from AMD by the Maifan stone and SRB immobilized particles prepared under these conditions were 92.12%, 95.93% and 87.14%, respectively, and the pH was increased from 4.08 to 7.49.

Received 29th November 2021
Accepted 24th January 2022

DOI: 10.1039/d1ra08709f

rsc.li/rsc-advances

1. Introduction

Acid mine drainage (AMD) has the characteristics of low pH value, and contains a large amount of heavy metal ions and SO_4^{2-}.[1] Direct discharge will damage the environment and threaten human health.[2] Currently, the methods commonly used for AMD treatment include the neutralization method,[3] adsorption method,[4] and microbial method.[5] The microbial method mainly uses the dissimilation and reduction effect of SRB to make the sulfide and heavy metals produced by it form a precipitate to achieve the purpose of removing heavy metal ions.[6] The microbial method mainly uses SRB to treat AMD, which can not only remove SO_4^{2-} but also produce alkalinity to improve the pH of waste, which has the advantages of easy access and low treatment cost.[7] Serrano[8] used SRB to remove As and Fe in AMD, with removal rates of 73% and 78%. Rodrigues[9] utilized shrimp shells as a treatment to biostimulate sulfate-reducing bacteria and remove metal ions in mine-impacted water (MIW). When Mingliang Zhang[10] treated AMD with prepared novel immobilized sulfate-reducing bacteria beads, the tolerance of SRB to heavy metals was significantly enhanced. According to research, microbial immobilization technology can improve the adaptability and impact resistance of bacteria in the pollution system, and maintain high biological activity.[11,12] The performance of the immobilized carrier is the key factor that determines the service life of the immobilized microorganism, the treatment effect and whether it can be industrialized.[13]

Maifan stone is a kind of natural ore; its main components are SiO_2, Al_2O_3, CaO, MgO, *etc.*, and it contains a variety of trace elements.[14] Maifan stone has the advantages of good adsorption performance, pH regulation and bioactive dissolution.[15] Hang

[a]*College of Mining, Liaoning Technical University, Fuxin 123000, Liaoning, China*
[b]*College of Science, Liaoning Technical University, Fuxin 123000, Liaoning, China*
[c]*College of Civil Engineering, Liaoning Technical University, Fuxin 123000, Liaoning, China*
[d]*Anshan Anqin Group, Anshan 114000, Liaoning, China*

Yang[16] used natural medical stone to adsorb humic acid (HA) in aqueous solution, and the results showed that the adsorption process was good, in line with the Langmuir model. At the same time, Maifan stone can release P, K, Na, Ca, Mg, Si, Mn and other macro and trace elements to promote the growth of microorganisms.[17] The results show that Maifan stone particles have better biological activity, chromium ion removal and pH adjustment. Jiang[18] prepared a moving bed biofilm reactor with Maifan stone, which was used for *in situ* remediation of polluted rivers. The results showed that the removal rate of chemical oxygen demand, ammonia nitrogen and total nitrogen of the moving bed biofilm reactor after adding Maifan stone were respectively increased by 4.86%, 8.89% and 9.01%. Therefore, the silicaluminate and silicate minerals in Maifan stone can not only adsorb pollutants, but also adjust the water pH value towards neutral so that SRB maintains good biological activity for the dissimilar reduction of SO_4^{2-} in AMD. At the same time, the release of Maifan stone K, Na, Ca, Mg elements can stimulate microbial growth. Maifan stone can be embedded in the preparation process of SRB immobilized particles to reduce the inhibition of SRB activity by high acidity and high concentration of metal ions. This enhances the biological activity of SRB, and improves the treatment effect of immobilized granules on AMD.

In this study, Maifan stone was used as an SRB carrier to prepare immobilized particles that were used to treat AMD. Maifan stone can not only solve the single adsorption of metal ions which cannot remove sulfate, but also solve the inhibition of SRB activity at low pH and high concentration of heavy metal ions. To ensure the adsorption by Maifan stone and SRB biological activity was maximized in the process of treating acid wastewater, the response surface method[19] was used to investigate the effects of Maifan stone dosage, Maifan stone particle size and SRB dosage on the treatment of AMD with Maifan stone and SRB immobilized particles, and the optimal preparation conditions were determined. This work is expected to provide a theoretical basis for the treatment of AMD with Maifan stone and SRB immobilized particles.

2. Materials and methods

2.1. Experimental materials

Maifan stone was taken from Mengyin County, Linyi City, Shandong Province. The Maifan stone was crushed and screened, and a sample with particle sizes ranging from 0.106–0.15 mm was selected. The samples were washed three times with deionized water to remove impurities and then dried at 105 °C.

SRB: activated sludge from the Xihe River, Fuxin City, Liaoning Province, was selected as the strain screening sample. According to Liu's[20] method, the bacteria mixed with SRB as the dominant strain were enriched by modified Postgate B medium for subsequent experiments.

AMD: based on the measured water quality data of mine water in a coal mining area of Fuxin City, Liaoning Province, the pH of simulated acid mine wastewater was set to 4, and the concentrations of SO_4^{2-}, Fe^{2+}, Mn^{2+}, Mg^{2+} and Ca^{2+} were 834.5 mg L^{-1}, 14 mg L^{-1}, 6 mg L^{-1}, 50 mg L^{-1}, and 50 mg L^{-1}, respectively.

All the chemicals selected for the experiments were analytical reagent grade.

2.2. Preparation of immobilized particles

Nine percent PVA (polyvinyl alcohol) and 0.5% SA (sodium alginate) were placed in a beaker and stirred until no bubbles existed. SA (0.5%) was added to the bacterial solution of SRB, which was stirred until sticky and set aside. Maifan stone and corn cobs were added to the gel, and the mixture was extracted by a syringe. The mixture was uniformly dripped into saturated boric acid solution (containing 2% $CaCl_2$, pH 6.0). After addition, the immobilized beads were cross-linked by stirring with a magnetic stirrer for 4 h and then cured.

2.3. Single factor test

The single factor test method was used to investigate the effect of the dosage of Maifan stone (1 g, 3 g, 5 g, 7 g, 9 g per 100 mL), the particle size of Maifan stone (0.150–0.270 mm, 0.106–0.150 mm, 0.075–0.106 mm, 0.058–0.075 mm and 0.048–0.058 mm) and the dosage of SRB (10 mL, 15 mL, 20 mL, 25 mL, 30 mL per 100 mL) on the removal rates of SO_4^{2-}, Fe^{2+} and Mn^{2+} and pH changes in the treatment of AMD with Maifan stone and SRB immobilized particles. The immobilized particles were added to 100 mL AMD according to a solid–liquid ratio of 1 : 10 (g mL^{-1}), and oscillated at a speed of 150 rpm. Sampling was carried out regularly every day. Each group of experiments was repeated 3 times, and the mean value was obtained. Based on the pH change of the wastewater and the removal rates of SO_4^{2-}, Fe^{2+} and Mn^{2+} as evaluation indicators, the optimal preparation conditions for Maifan stone and SRB immobilized particles were determined.

2.4. Response surface test

Based on the single factor experiment, the response surface optimization test of the Box–Behnken model is used, and the response surface test is carried out with the removal rates of SO_4^{2-}, Fe^{2+} and Mn^{2+} and pH value as the response values. Each group of experiments was repeated three times, and the data were analyzed using Design Expert 8.0 software. The coding and level of test factors are shown in Table 1.

2.5. Water quality testing method

Fe^{2+} concentrations were determined using *o*-phenanthroline spectrophotometry (HJ/T 345-2007), the wavelength was

Table 1 Response surface test factors and level design

		Level		
Factor	Coding	−1	0	1
Addition of Maifan stone (g per 100 mL)	X1	3	5	7
Maifan stone particle size (mm)	X2	0.06	0.09	0.12
SRB dosing amount (mL per 100 mL)	X3	20	25	30

measured at 510 nm. Mn^{2+} content was determined using potassium periodate spectrophotometry (GB 11906-89), the wavelength was measured at 525 nm. SO_4^{2-} content was determined using barium chromate spectrophotometry (HJ/T 342-2007), the wavelength was measured at 420 nm. pH was determined with the glass electrode method (GB 6920-86).

3. Experimental results and discussion

3.1. Single factor test analysis

The effect of the dosage of Maifan stone on the removal rates of SO_4^{2-}, Fe^{2+}, Mn^{2+} and pH increase in AMD is shown in Fig. 1. It can be seen from Fig. 1 that when the dosage of SRB is 25 mL per 100 mL and the particle size of Maifan stone is 0.075–0.106 mm, with the increase in time, the removal rates of SO_4^{2-}, Fe^{2+}, Mn^{2+} and pH increase in AMD. The effect is gradually strengthening, but the increase is reduced. When the dosage of Maifan stone is 5 g per 100 mL, the highest removal rates of SO_4^{2-}, Fe^{2+} and Mn^{2+} after the prepared Maifan stone is combined with SRB immobilized particles to treat AMD are 87.10%, 87.45% and 74.68%, respectively. The pH value of the wastewater rose from 4.08 to 7.55. When the dosage of Maifan stone is more than 7 g, the effect of treating AMD begins to weaken. This is because when the dosage of Maifan stone is greater than 7 g, the prepared particles have a higher viscosity, the quality of the immobilized particles is reduced, and aggregation is prone to occur during the treatment of AMD, so the specific surface area of the material is reduced, which affects the fixation and adsorption of ions to the chemical particles.

The effect of Maifan stone particle size on the removal rates of SO_4^{2-}, Fe^{2+}, Mn^{2+} and pH increase in AMD is shown in Fig. 2. It can be seen from Fig. 2 that when SRB dosage is 25 mL per 100 mL and Maifan stone dosage is 5 g per 100 mL, with the increase in Maifan stone particle size, the removal rates of SO_4^{2-}, Fe^{2+}, Mn^{2+} and pH enhancement effect in AMD increase first and then decrease. This is because the Maifan stone has certain pores.[21] After crushing and sieving, the particle size is reduced, the specific surface area is increased, and the adsorption capacity for pollutants is enhanced, which reduces the inhibition by harmful toxins in the wastewater to the biological activity of SRB. At the same time, the Maifan stone can release beneficial trace elements and promote the growth of SRB in the immobilized particles.[22] However, when the particle size of Maifan stone is too small (0.058–0.075 mm, 0.048–0.058 mm), the prepared immobilized particles will easily float on the water surface and will not settle easily in the process of treating AMD, which will affect the removal effect. When the particle size of the Maifan stone is too large (0.150–0.270 mm, 0.106–0.150 mm), the specific surface area of the Maifan stone is relatively reduced, and the ability to activate SRB decreases. When the particle size of Maifan stone is 0.075–0.106 mm, the highest removal rates of SO_4^{2-}, Fe^{2+}, Mn^{2+} in AMD are 91.23%, 92.05%,

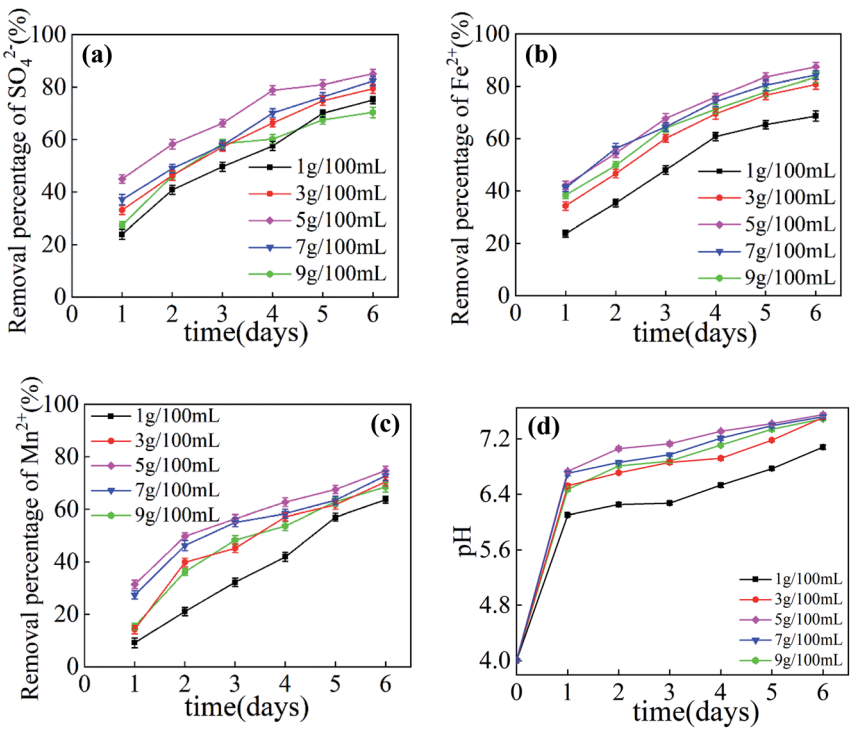

Fig. 1 The influence of the dosage of Maifan stone on the removal rates of SO_4^{2-}, Fe^{2+}, Mn^{2+} and the effect on pH improvement in AMD. (a) The influence of the dosage of Maifan stone on the removal rate of SO_4^{2-}. (b) The influence of the added amount of Maifan stone on Fe^{2+} removal rate. (c) The influence of the dosage of Maifan stone on the removal rate of Mn^{2+}. (d) The influence of the dosage of Maifan stone on the effect of increasing pH.

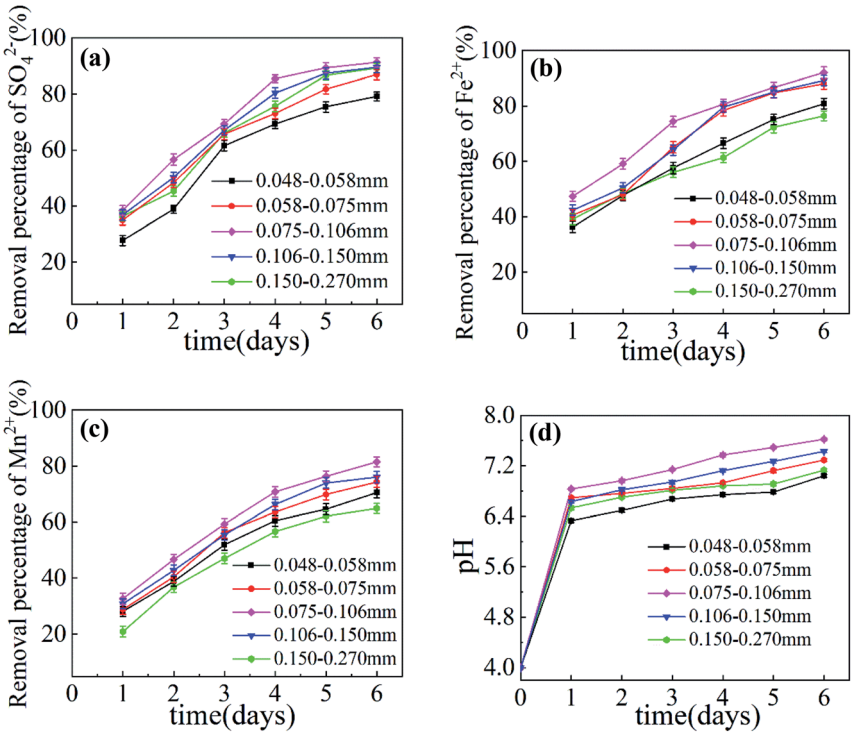

Fig. 2 The effect of Maifan stone particle size on the removal rates of SO_4^{2-}, Fe^{2+}, Mn^{2+} and the effect on pH improvement in AMD. (a) The effect of Maifan stone particle size on SO_4^{2-} removal rate. (b) The effect of Maifan stone particle size on Fe^{2+} removal rate. (c) The effect of Maifan stone particle size on Mn^{2+} removal rate. (d) The effect of Maifan stone particle size on the enhancement of pH.

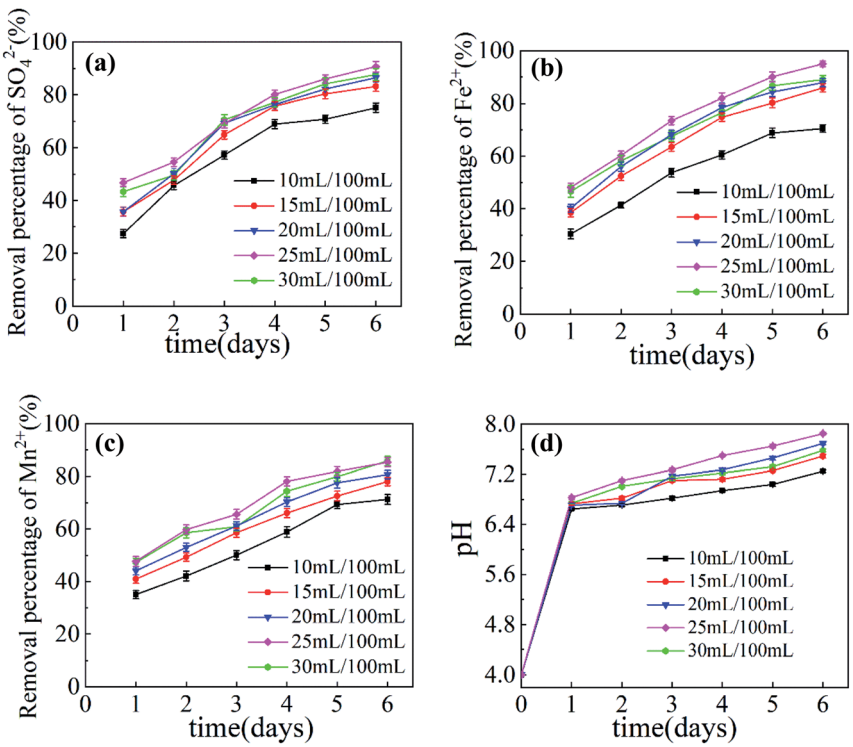

Fig. 3 The influence of the dosage of SRB on the removal rates of SO_4^{2-}, Fe^{2+}, Mn^{2+} and the effect on pH improvement in AMD. (a) The influence of SRB dosage on SO_4^{2-} removal rate. (b) The influence of SRB dosage on Fe^{2+} removal rate. (c) The influence of SRB dosage on the removal rate of Mn^{2+}. (d) The influence of SRB dosage on the effect of pH improvement.

and 81.50%, respectively, and the pH value of the wastewater rises from 4.08 to 7.62. Comparing with Maifan stones of other particle sizes, Maifan stones prepared with 0.075–0.106 mm Maifan stones combined with SRB immobilized particles have the best repair effect on AMD.

The influence of SRB dosage on SO_4^{2-}, Fe^{2+}, Mn^{2+} removal rates and pH increase in AMD is shown in Fig. 3. It can be seen from Fig. 3 that when the dosage of Maifan stone is 5 g per 100 mL, the particle size of Maifan stone is 0.075–0.106 mm, and the dosage of SRB is within the range of 10 mL per 100 mL to 25 mL per 100 mL, with the increase in SRB dosage, the repairing effect of immobilized particles on AMD shows a gradually strengthening trend. This is because SRB reduces SO_4^{2-} in wastewater to H_2S, and Fe^{2+}, Mn^{2+} react with it to form sulfide precipitates and are removed.[23,24] In this process, the pH value of wastewater increases. In addition, Fe^{2+} and Mn^{2+} will be removed due to the biological adsorption, precipitation and adsorption of the Maifan stone of SRB.[25,26] When the dosage of SRB is 10 mL, the remediation of pollutants effect in AMD is poor, because when the dosage of SRB is small, the activity of immobilized particles is lower.[27] When the dosage of SRB was 30 mL, the repairing effect in AMD began to decline, and with the increase in SRB content, the preparation of immobilized particles became more difficult. The research showed that the greater the amount of SRB, the worse the diffusibility of the particles. Larger SRB dosage will cause a waste of raw materials, so the experiment gives the SRB dosage as 25 mL per 100 mL.

3.2. Response surface test analysis

The Box–Behnken model response surface test plan and results are shown in Table 2. The multiple regression equation was fitted using Design Expert 8.0 software, and the analysis of variance was carried out to obtain the treatment effect of Maifan stone and SRB immobilized particles on AMD under the three factors of Maifan stone dosage, Maifan stone particle size and SRB dosage.

According to the analysis of variance and significance check of the regression model, the F values of the variance test of SO_4^{2-}, Fe^{2+} and Mn^{2+} removal rates and pH change regression model were 48.81, 8.43, 34.35 and 202.61 respectively. The p values were <0.0001, 0.0051, <0.0001 and <0.0001, all less than 0.01, indicating that the model reached a significance level:[28] it is statistically significant and can be used to replace the real points of the test for result analysis. The multivariate correlation coefficients R^2 of the four models are 0.9843, 0.9155, 0.9779 and 0.9962, and the correction coefficients of determination R_{adj}^2 are 0.9641, 0.8069, 0.9494 and 0.9913, respectively, indicating that the four models can explain 96.41%, 80.69%, 94.94% and 99.13%, respectively. It further shows that the goodness of fit of the regression model is good. The model can analyze and optimize the removal rates of SO_4^{2-}, Fe^{2+} and Mn^{2+} and pH changes.

3.2.1. Removal percentage of SO_4^{2-}. It can be seen from Fig. 4(a) that the interaction between the particle size of Maifan stone and the dosage of SRB has no significant effect on the SO_4^{2-} removal rate ($p = 0.0002 < 0.05$). In the selected experimental range, the removal rate of SO_4^{2-} increased first and then decreased with the increase in Maifan stone particle size, and gradually decreased with the increase in SRB dosage. It can be seen from Fig. 4(b) that the interaction between the dosage of Maifan stone and the dosage of SRB had a significant effect on the removal rate of SO_4^{2-}. The effect of SRB dosage on SO_4^{2-} removal was dominant among the two factors. It can be seen from Fig. 4(c) that the interaction between the dosage of Maifan stone and the particle size of Maifan stone has a significant impact on the SO_4^{2-} removal rate ($p = 0.0025 < 0.05$), and the dosage of Maifan stone plays a dominant role in the two factors. In the selected experimental range, the SO_4^{2-} removal rate decreased first with the increase in Maifan stone particle size.

Table 2 Experimental design factors and results[a]

Number	X_1	X_2	X_3	SO_4^{2-} removal rate (%)	Fe^{2+} removal rate (%)	Mn^{2+} removal rate (%)	pH value
1	5.00	0.09	25.00	92.22	95.41	86.05	7.45
2	3.00	0.09	30.00	88.59	92.75	74.73	6.94
3	5.00	0.09	25.00	92.22	95.41	86.05	7.45
4	5.00	0.12	20.00	93.19	93.16	77.23	6.61
5	7.00	0.09	20.00	89.73	94.29	83.75	6.73
6	3.00	0.09	20.00	91.25	89.45	74.31	6.48
7	5.00	0.09	25.00	92.22	95.41	86.05	7.45
8	3.00	0.12	25.00	91.41	90.75	71.2	6.68
9	5.00	0.06	20.00	93.24	93.18	74.98	6.67
10	5.00	0.06	30.00	93.17	93.28	78.21	6.97
11	5.00	0.09	25.00	92.22	95.41	86.05	7.45
12	3.00	0.06	25.00	90.44	84.92	69.78	6.48
13	5.00	0.09	25.00	92.22	95.41	86.05	7.45
14	7.00	0.06	25.00	92.18	94.19	82.11	6.66
15	7.00	0.09	30.00	90.53	94.38	84.36	6.99
16	7.00	0.12	25.00	90.85	94.25	82.3	6.8
17	5.00	0.12	30.00	93.09	93.56	82.11	7.27

[a] Notes: X_1 is the dosage of Maifan stone, g per 100 mL; X_2 is the particle size of Maifan stone, mm; X_3 is the dosage of SRB, mL per 100 mL.

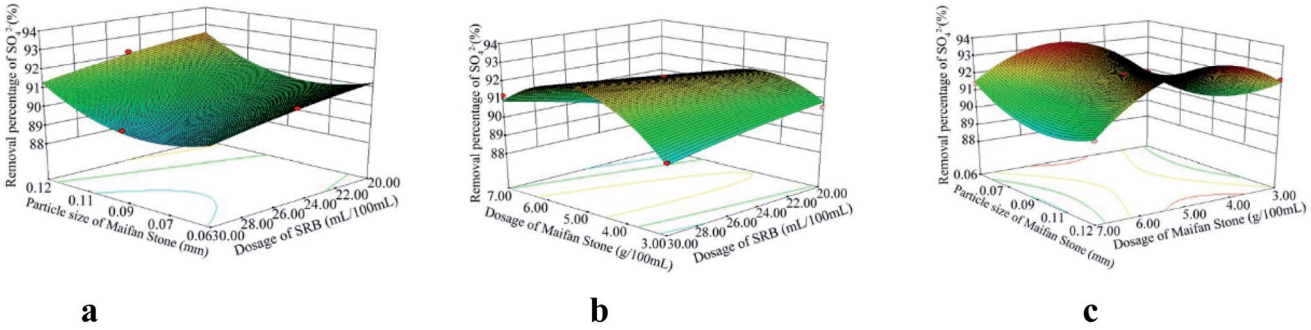

Fig. 4 Response surface plots of SO_4^{2-} removal rate under the interaction of various factors. (a) SO_4^{2-} removal rate under the interaction of Maifan stone particle size and SRB dosage. (b) SO_4^{2-} removal rate under the interaction of Maifan stone dosage and SRB dosage. (c) SO_4^{2-} removal rate under the interaction of Maifan stone particle size and Maifan stone dosage.

With the increase in Maifan stone dosage, it first increases and then decreases. The removal of SO_4^{2-} from AMD mainly uses the dissimilative reduction effect of SRB to reduce sulfate to soluble sulfides (H_2S, HS^- and S^{2-}) through bioenergy metabolism, and reaction with metals to form metal sulfide precipitation.[29] At the same time, the alkalinity released by Maifan stone neutralizes the pH value, which is conducive to the precipitation of metal carbonate minerals.

3.2.2. Removal percentage of Fe^{2+}. It can be seen from Fig. 5(a) that the interaction between Maifan stone particle size and SRB dosage has no significant effect on Fe^{2+} removal rate ($p = 0.0462 < 0.05$). Within the selected experimental range, the Fe^{2+} removal rate first increases and then decreases with the increase in Maifan stone particle size, and gradually increases with the increase in SRB dosage. It can be seen from Fig. 5(b) that the interaction between Maifan stone dosage and SRB dosage has no significant effect on Fe^{2+} removal rate ($p = 0.0462 < 0.05$). Within the selected experimental range, the Fe^{2+} removal rate gradually increases with the increase in Maifan stone dosage and SRB dosage. Fe^{2+} was removed because the Maifan stone has a tetrahedral crystal structure based on siloxy $[SiO_4]^{4-}$, and Mg^{2+}, Na^+, K^+, Ca^{2+} plasmons are combined at its ends through ionic bonds. When the Maifan stone is in an aqueous environment, it can be partially ionized to form a large number of active groups $[-SiO]^-$ to capture heavy metal ions in the water.[30] SRB produces S^{2-} (ref. 31) due to the reduction[32] of SO_4^{2-}, which forms a precipitate with Fe^{2+}. Additionally, the removal of Fe^{2+} was enhanced because the negative charge on the surface of SRB[33] facilitates electrostatic adsorption of Fe^{2+}, and the sulfate-reducing bacterium extracellular polymer also affects biological flocculation of Fe^{2+}.[34] It can be seen from Fig. 5(c) that the interaction between Maifan stone dosage and Maifan stone particle size has a significant effect on the Fe^{2+} removal rate ($p = 0.0462 < 0.05$), and the effect of Maifan stone dosage on Fe^{2+} removal dominates the two factors. Within the selected experimental range, the Fe^{2+} removal rate increases with the addition of Maifan stone, the increase in the amount gradually increases, and gradually increases with the increase in the dosage of Maifan stone.

3.2.3. Removal percentage of Mn^{2+}. It can be seen from Fig. 6(a) that the interaction between Maifan stone particle size and SRB dosage has no significant effect on the Mn^{2+} removal rate ($p = 0.0462 < 0.05$). Within the selected experimental range, the Mn^{2+} removal rate first increases and then decreases with the increase in Maifan stone particle size, and the Mn^{2+} removal rate gradually decreases with the increase in SRB dosage. The removal of Mn^{2+} mainly relies on the adsorption by Maifan stone. At the same time, SRB will reduce SO_4^{2-} to S^{2-}, which combines with Mn^{2+} to form MnS precipitation to achieve the purpose of removal.[35] It can be seen from Fig. 6(b) that the interaction between Maifan stone dosage and SRB dosage has no significant effect on Mn^{2+} removal rate ($p = 0.0462 < 0.05$).

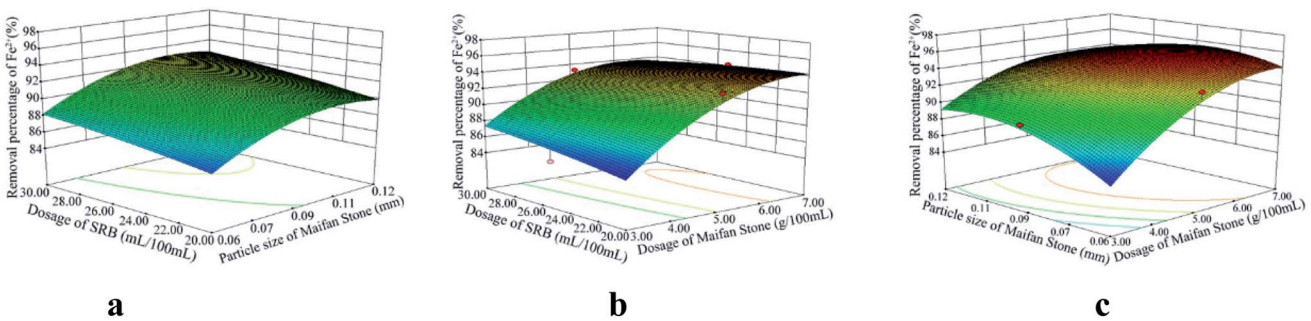

Fig. 5 Response surface plots of Fe^{2+} removal rate under the interaction of various factors. (a) Fe^{2+} removal rate under the interaction of Maifan stone particle size and SRB dosage. (b) Fe^{2+} removal rate under the interaction of Maifan stone dosage and SRB dosage. (c) Fe^{2+} removal rate under the interaction of Maifan stone dosage and Maifan stone particle size.

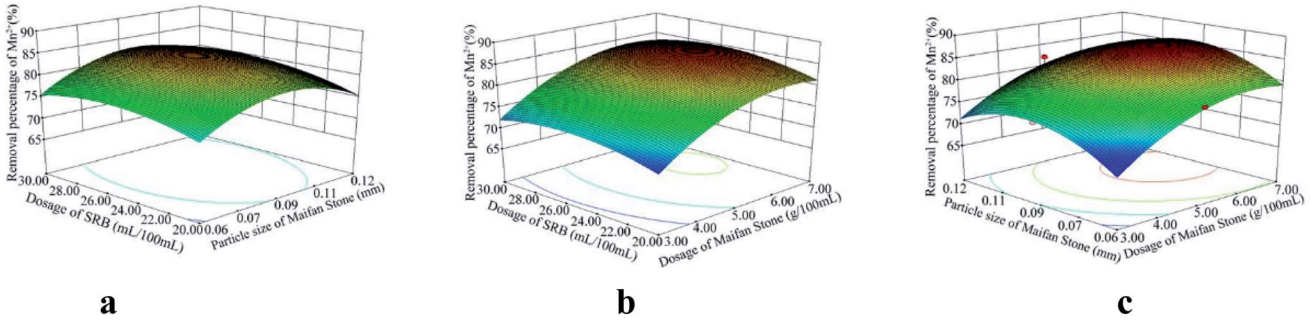

Fig. 6 Response surface plots of Mn^{2+} removal rate under the interaction of various factors. (a) Mn^{2+} removal rate under the interaction of Maifan stone particle size and SRB dosage. (b) Mn^{2+} removal rate under the interaction of Maifan stone dosage and SRB dosage. (c) Mn^{2+} removal rate under the interaction of Maifan stone dosage and Maifan stone particle size.

Within the selected experimental range, the Mn^{2+} removal rate gradually increases with the increase in SRB dosage and increases with the increase in Maifan stone dosage. It can be seen from Fig. 6(c) that the interaction between Maifan stone dosage and Maifan stone particle size has no significant effect on Mn^{2+} removal rate ($p = 0.0462 < 0.05$). Within the selected experimental range, the Mn^{2+} removal rate first increases and then decreases with the increase in Maifan stone particle size, and gradually increases with the increase in Maifan stone dosage.

3.2.4. pH improvement. It can be seen from Fig. 7(a) that the interaction between the particle size of Maifan stone and the dosage of SRB has a significant effect on the increase of pH ($p = 0.0013 < 0.05$), and the effect of the dosage of SRB on the increase of pH accounts for the two factors leading position. It shows that in the presence of SRB, within a certain range, the smaller the particle size of Maifan stone, the more pores and the larger the specific surface area, so the pH value of wastewater will be effectively increased. The main factor of pH increase in the system is the bidirectional adjustment ability of Maifan stone.[36] Because direct treatment of wastewater by SRB consumed H^+ and the pH of the wastewater increased significantly.[37] Simultaneously, SRB decomposes the carbon source in the environment to produce HCO_3^- through biological metabolism, which increases the pH value and alkalinity of the solution. It can be seen from Fig. 7(b) that the interaction between Maifan stone dosage and SRB dosage has a significant impact on pH improvement ($p = 0.0237 < 0.05$), and SRB dosage plays a dominant role in the two factors. The dominant position indicates that Maifan stone and SRB co-process AMD. Maifan stone can release factors that contribute to the growth of SRB, increase the reduction ability of SRB, and thus increase the pH value to improve the quality of the water environment. It can be seen from Fig. 7(c) that the interaction between the dosage of Maifan stone and the particle size of Maifan stone has no significant effect on the increase of pH ($p = 0.0462 < 0.05$). With the increase in the dosage of diameter and Maifan stone, the pH value of wastewater will be effectively improved.

Using the optimization function of Design-Expert, on the basis of ensuring the maximum increase in SO_4^{2-}, Fe^{2+}, Mn^{2+} removal rates and pH value in AMD, predicts the optimal preparation conditions of Maifan stone and SRB immobilized particles. The predicted calculation results are as follows: the dosage of Maifan stone is 5.44 g, the particle size of Maifan stone is 0.09 mm, and the dosage of SRB is 26.75 mL per 100 mL. According to the feasibility of the test, the test results were adjusted to some extent, and the optimal preparation conditions for the Maifan stone and SRB immobilized particles were finally determined as the Maifan stone dosage is 5 g, the Maifan stone particle size is 0.075–0.106 mm, and the SRB dosage is 5 g. The dosage is 25 mL per 100 mL. Through experimental inspection, under these preparation conditions, the removal rates of SO_4^{2-}, Fe^{2+} and Mn^{2+} are 92.12%, 95.93%, and 87.14%, respectively, and the pH is increased from 4.08 to 7.49. The

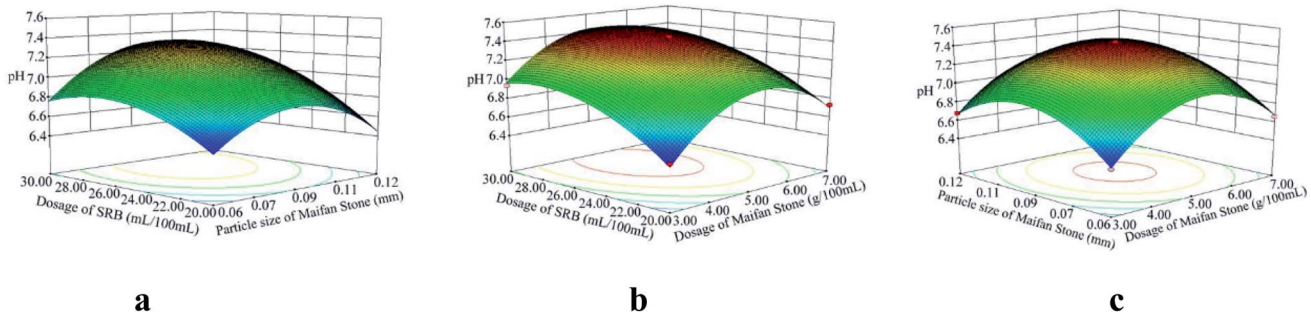

Fig. 7 Response surface plots of pH changes under the interaction of various factors. (a) pH enhancement effect under the interaction of Maifan stone particle size and SRB dosage. (b) pH enhancement effect under the interaction of Maifan stone dosage and SRB dosage. (c) pH enhancement effect under the interaction of Maifan stone dosage and Maifan stone particle size.

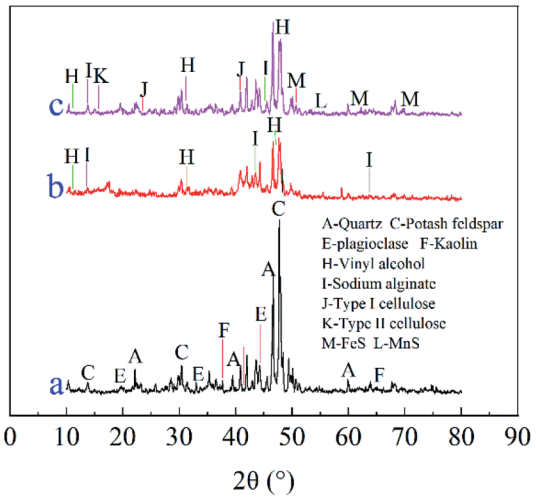

Fig. 8 XRD patterns of Maifan stone combined with SRB before and after AMD repair. (a) Shandong Maifan stone; (b) before treatment of AMD with Maifan stone sulfate-reducing bacterium-immobilized particles; (c) after treatment of AMD with Maifan stone sulfate-reducing bacterium-immobilized particles.

errors are all within the allowable range, which indicates that the predicted value of the model is in good agreement with the actual test value. It further shows that the model can truly and accurately analyze and predict the experimental results of Maifan stone and SRB immobilized particles in the treatment of AMD, which has practical value.

4. Mechanistic analysis of AMD mitigation by Maifan stones combined with SRB

4.1. XRD analysis

Fig. 8 shows the XRD data for Shandong Maifan stone, and Maifan stone–sulfate-reducing bacterium-immobilized particles before and after AMD mitigation.

Fig. 8(a) shows that Maifan stone–sulfate-reducing bacterium immobilized particles exhibit peak characteristics of Maifan stone, such as those for quartz and potash feldspar, plagioclase, kaolin, PVA and SA.[38] Typical characteristic peaks of type I cellulose and type II cellulose,[39,40] MnS and FeS peaks appeared after AMD was treated by the immobilized granules. Typical peaks characteristic of type I cellulose and type II cellulose appeared after AMD was treated with the immobilized particles indicating that the corncobs carbon source slowly released organic matter for the growth and metabolism of SRB.

The occurrence of MnS and FeS peaks is due to the SRB inside the particles making SO_4^{2-} become the electron acceptor. The receiving electrons are reduced to S^{2-} and OH^- products, and some of the Fe^{2+} and Mn^{2+} ions generate precipitation with the reduction products and are removed.

4.2. SEM analysis

Shandong Maifan stone and the insides of Maifan stone–SRB immobilized particles before and after AMD treatment are shown in Fig. 9.

Fig. 9(b) shows that the surface texture of Maifan stone–SRB immobilized particles before AMD treatment is relatively smooth, does not contain large raised folds, and the pore size is uniform and suitable. Fig. 9(c) shows that after the treatment of AMD by Maifan stone–SRB immobilized particles, some of the surface pores became smaller and uneven, and a large number of small particles were deposited. It shows that the SO_4^{2-} removal by immobilized particles occurs simultaneously on the surface and inside. SO_4^{2-} moves from the outside to the inside through the pores, after SRB dissimilation reduction and removal, the sulfide precipitates are finally formed in the particles. Sulfide precipitates cause internal impurities to increase, pores become smaller, or even clogged. At the same time, many raised folds are formed. The folds are caused because Mn^{2+} adsorbed on the surface is toxic to SRB.[41]

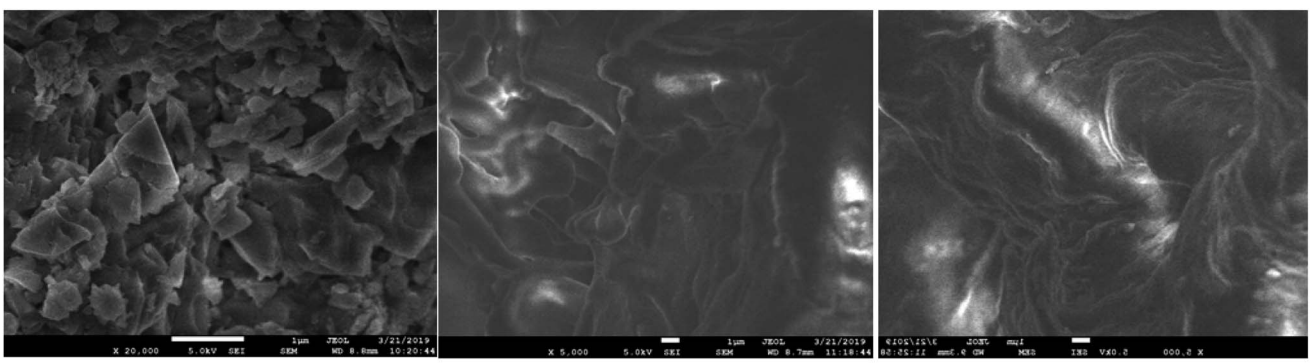

Fig. 9 SEM images of Maifan stones combined with SRB before and after AMD repair.

5. Conclusions

(1) XRD and SEM analysis before and after treatment of AMD by Maifan stone–SRB immobilized particles showed that immobilized particles can effectively remove SO_4^{2-}, Fe^{2+} and Mn^{2+} from AMD.

(2) The single factor experiment determined the preparation conditions of Maifan stone and SRB immobilized particles: the dosage of Maifan stone was 5 g, the particle size of Maifan stone was 0.075–0.106 mm, and the dosage of SRB was 25 mL per 100 mL.

(3) The response surface method established the prediction models of SO_4^{2-} removal rate, Fe^{2+} removal rate, Mn^{2+} removal rate and pH increase. The correlation coefficients of the models are 0.9843, 0.9155, 0.9779 and 0.9962 respectively. The model fits well and the experimental error is small. The Maifan stone under the conditions of different dosages of Maifan stone, Maifan stone pellets, and SRB dosages was combined with SRB immobilized particles to remove SO_4^{2-}, Fe^{2+} and Mn^{2+} from AMD and provide pH improvement.

(4) The response surface experimental model predicts that the optimal preparation conditions of Maifan stone and SRB immobilized particles are as follows: Maifan stone dosage is 5 g, Maifan stone particle size is 0.075–0.106 mm, and SRB dosage is 25 mL per 100 mL. The experimental results of the treatment of AMD with Maifan stone prepared under these conditions in conjunction with SRB immobilized particles showed that the removal rates of SO_4^{2-}, Fe^{2+} and Mn^{2+} were 92.12%, 95.93% and 87.14%, respectively, and the pH value increased from 4.08 to 7.49. The errors are within the allowable range, indicating that the model is accurate and reliable.

Author contributions

Xuying Guo and Zhiyong Hu: conception. Zhiyong Hu: writing – original draft. Saiou Fu and Ying Li: data curation. Xuying Guo and Yanrong Dong: writing – review & editing.

Conflicts of interest

The authors declare no conflict of interest.

Acknowledgements

The project is funded by the National Natural Science Foundation of China (51304114), Department of Education of Liaoning Province (LJ2017FAL016, LJKZ0340).

References

1 D. Hou, P. Zhang, D. Wei, *et al.*, Simultaneous removal of iron and manganese from acid mine drainage by acclimated bacteria, *J. Hazard. Mater.*, 2020, **396**, 122631.
2 M. Sharma, M. Poddar, Y. Gupta, S. Nigam, *et al.*, Solar light assisted degradation of dyes and adsorption of heavy metal ions from water by CuO–ZnO tetrapodal hybrid nanocomposite, *Mater. Today Chem.*, 2020, **17**, 100336.
3 B. S. Acharya and G. Kharel, Acid mine drainage from coal mining in the United States – an overview, *J. Hydrol.*, 2020, **588**, 125061.
4 R. Markovic, M. Bessho, N. Masuda, *et al.*, New Approach of Metals Removal from Acid Mine Drainage, *Appl. Sci.*, 2020, **10**(17), 5925.
5 Y. Sato, T. Hamai, T. Hori, *et al.*, Optimal start-up conditions for the efficient treatment of acid mine drainage using sulfate-reducing bioreactors based on physicochemical and microbiome analyses, *J. Hazard. Mater.*, 2022, **423**, 127089.
6 H. Lin, Z. Li and Y. He, Advances in Treatment of Acid Mine Drainage by Sulfate-Reducing Bacteria, *Environ. Prot. Sci.*, 2019, **45**(05), 25–31.
7 M. D. Ruehl and S. R. Hiibel, Evaluation of organic carbon and microbial inoculum for bioremediation of acid mine drainage, *Miner. Eng.*, 2020, **157**, 106554.
8 J. Serrano and E. Leiva, Removal of arsenic using acid/metal-tolerant sulfate reducing bacteria: A new approach for bioremediation of high-arsenic acid mine waters, *Water*, 2017, **9**(12), 994.
9 C. Rodrigues, D. Núez-Gómez, H. Follmann, *et al.*, Biostimulation of sulfate-reducing bacteria and metallic ions removal from coal mine-impacted water (MIW) using shrimp shell as treatment agent, *J. Hazard. Mater.*, 2020, **398**, 122893.
10 M. Zhang, H. Wang and X. Han, Preparation of metal-resistant immobilized sulfate reducing bacteria beads for acid mine drainage treatment, *Chemosphere*, 2016, **154**, 215–223.
11 S. Sun, S. Fan, K. Shen, *et al.*, Laboratory assessment of bioleaching of shallow eutrophic sediment by immobilized photosynthetic bacteria, *Environ. Sci. Pollut. Res.*, 2017, **24**, 22143–22151.
12 Y. Pei, X. Wu, G. Xu, *et al.*, Tannin-immobilized cellulose microspheres as effective adsorbents for removing cationic dye (Methylene Blue) from aqueous solution, *J. Chem. Technol. Biotechnol.*, 2017, **92**, 1276–1284.
13 Y. Zhang, Z. Yu, Y. Hu, *et al.*, Immobilization of nitrifying bacteria in magnetic PVA–SA-diatomite carrier for efficient removal of NH_4^+–N from effluents, *Environ. Technol. Innovat.*, 2021, **22**, 101407.
14 X. H. Liu, J. X. Fu, L. Li, *et al.*, Leaching Mineral Elements from Chinese Maifan-Stone, *Adv. Mater. Res.*, 2008, **58**, 69–75.
15 J. Ou, H. Li, Z. Yan, *et al.*, *In situ* immobilisation of toxic metals in soil using Maifan stone and illite/smectite clay, *Sci. Rep.*, 2018, **8**(1), 4618.
16 H. Yang, B. Luo, Y. Zhang, *et al.*, Study of Humic Acid Adsorption Character on Natural Maifan Stone: Characterization, Kinetics, Adsorption Isotherm, and Thermodynamics, *ACS Omega*, 2020, **5**, 7683–7692.
17 X. Li and H. Peng, Influence of different leaching conditions on dissolution performance of medical stone, *Environ. Sci. Technol.*, 2021, **44**(01), 13–23.
18 H. Jiang, Z. Zhang, Z. Lin, X. Gong, *et al.*, Modification of polyurethane sponge filler using medical stones and application in a moving bed biofilm reactor for ex situ

remediation of polluted rivers, *J. Water Process Eng.*, 2021, **42**, 102189.

19 J. Cao, Y. Wu, Y. Jin, P. Yilihan and W. Huang, Response surface methodology approach for optimization of the removal of chromium (VI) by NH_2-MCM-41, *J. Taiwan Inst. Chem. Eng.*, 2014, **45**(3), 860–868.

20 F. Liu, G. Zhang, S. Liu, *et al.*, Bioremoval of arsenic and antimony from wastewater by a mixed culture of sulfate-reducing bacteria using lactate and ethanol as carbon sources, *Int. Biodeterior. Biodegrad.*, 2018, **126**, 152–159.

21 J. Li, *et al.*, Chemical properties of Maifan Stone and its application in water quality optimization, *Environ. Sci. Technol.*, 2008, 63–66+75.

22 P. Ma, Nitrate removal from groundwater using medical stone as carrier, PhD thesis, China University of Geosciences, Beijing, 2013.

23 B. Anandkumar and R. George, Corrosion behavior of SRB Desulfobulbus propionicus isolated from an Indian petroleum refinery on mild steel, *Mater. Corros.*, 2012, **63**(4), 355–362.

24 M. G. Kiran, K. Pakshirajan and G. Das, Heavy metal removal from multicomponent system by sulfate reducing bacteria: mechanism and cell surface characterization, *J. Hazard. Mater.*, 2017, **324**, 62–70.

25 H. Lin, Z. Li and Y. He, Advances in Treatment of Acid Mine Drainage by Sulfate-Reducing Bacteria, *Environ. Prot. Sci.*, 2009, **45**(05), 25–31.

26 M. Vossoughi, M. Shakeri and I. Alemzadeh, Performance of anaerobic baffled reactor treating synthetic wastewater influenced by decreasing COD/SO_4 ratios, *Chem. Eng. Process.*, 2003, **42**(10), 811–816.

27 Y. Miao, S. Qi and J. Chen, Application of sulfate reducing bacteria in the treatment of acid mine wastewater, *Appl. Chem. Ind.*, 2021, **50**(11), 3074–3078+3086.

28 Y. Chao, B.-G. Liu and P. J. Hui, Optimization of Calcination with Basic Cobalt Carbonate for Preparation of Co_3O_4 by Response Surface Methodology, *Min. Metall. Eng.*, 2021, **41**(01), 114–118.

29 C.-M. Neculita, G. J. Zagury and B. Bussière, Passive Treatment of Acid Mine Drainage in Bioreactors using Sulfate-Reducing Bacteria: Critical Review and Research Needs, *J. Environ. Qual.*, 2007, **36**(1), 1–16.

30 J. Lv, Y. Zhao and R. Zhao, Absorption of copper, zinc and cadmium on MF (Granite) in sea water a aqueous solution, *J. Fish. Sci. China*, 2000, **7**(1), 87–89.

31 B. Anandkumar, *et al.*, Corrosion behavior of SRB Desulfobulbus propionicus isolated from an Indian petroleum refinery on mild steel, *Mater. Corros.*, 2012, **63**(4), 355–362.

32 M. G. Kiran, K. Pakshirajan and G. Das, Heavy metal removal from multicomponent system by sulfate reducing bacteria: Mechanism and cell surface characterization, *J. Hazard. Mater.*, 2017, **324**, 62–70.

33 H. Lin, *et al.*, Advances in Treatment of Acid Mine Drainage by Sulfate-Reducing Bacteria, *Environ. Prot. Sci.*, 2019, **45**(05), 25–31.

34 M. Vossoughi, M. Shakeri and I. Alemzadeh, Performance of anaerobic baffled reactor treating synthetic wastewater influenced by decreasing COD/SO_4 ratios, *Chem. Eng. Process.*, 2003, **42**(10), 811–816.

35 K. B. Hallberg and D. B. Johnson, Biological manganese removal from acid mine drainage in constructed wetlands and prototype bioreactors, *Sci. Total Environ.*, 2005, **338**(1–2), 115–124.

36 F. Han, *et al.*, Effects of maifanite on growth, physiological and phytochemical process of submerged macrophytes Vallisneria spiralis, *Ecotoxicol. Environ. Saf.*, 2020, **189**, 109941.

37 X. Li, *et al.*, The bioenergetics mechanisms and applications of sulfate-reducing bacteria in remediation of pollutants in drainage: A review, *Ecotoxicol. Environ. Saf.*, 2018, **158**, 162–170.

38 Q. Wang, *et al.*, Alginate/polyethylene glycol blend fibers and their properties for drug controlled release, *J. Biomed. Mater. Res., Part A*, 2007, **82**(1), 122–128.

39 W. P. F. Neto, *et al.*, Extraction and characterization of cellulose nanocrystals from agro-industrial residue–Soy hulls, *Ind. Crops Prod.*, 2013, **42**, 480–488.

40 H. A. Silvério, *et al.*, Extraction and characterization of cellulose nanocrystals from corncob for application as reinforcing agent in nanocomposites, *Ind. Crops Prod.*, 2013, **44**, 427–436.

41 Y. Zhang, *Conversion of Hemicellulose into Furfural Using Inorganic Salt Catalysts [D]*, An Hui University of Science and Technology, 2014.